Low Temperature Physics/Fizika Nizkikh Temperatur, 2014, v. 40, No. 3, pp. 309–316

Low-temperature ^{1}H NMR spectroscopic study of hydration properties of a hybrid system based on nanosilica, DNA and doxorubicin in the presence of C_{60} fullerene

V.V. Turov[1], Yu.I. Prylutskyy[2], A.P. Ugnivenko[1], V.N. Barvinchenko[1], T.V. Krupskaya[1], N.G. Tsierkezos[3], and U. Ritter[3]

[1]*O.O. Chuiko Institute of Surface Chemistry of NAS of Ukraine, 17 Gen. Naumov Str., Kyiv 03680, Ukraine*

[2]*Taras Shevchenko National University of Kyiv, 64 Volodymyrska Str., Kyiv 01601, Ukraine*
E-mail: prylut@ukr.net

[3]*Technical University of Ilmenau, 25 Weimarer Str., Ilmenau 98693, Germany*

Received August 14, 2013, revised September 5, 2013

The structure of hydrate cover layers of SiO_2–DNA–Dox (where Dox: doxorubicin) and SiO_2–DNA–Dox–C_{60} fullerene hybrids was studied by means of low-temperature ^{1}H NMR spectroscopy in tetrachloromethane. The hydration properties of SiO_2–DNA–Dox nanomaterials combined with fullerenes and their derivatives are extremely important for their further use as therapeutics in cancer treatment and for safety reasons. The findings reveal that the hydration properties of the hybrids differ from those of the solid DNA particulates or SiO_2–DNA systems due to the existence of different types of water clusters, namely the weakly- (WAW) and strongly-associated water (SAW) clusters. For SAW clusters the radial distributions as well as the distributions of change in Gibbs free energy due to adsorptive interactions at the surfaces of the investigated systems were obtained.

PACS: 61.05.Qr Magnetic resonance techniques; Mössbauer spectroscopy (for structure determination only);
61.46.–w Structure of nanoscale materials;
82.56.Ub Structure determination with NMR.

Keywords: SiO_2–DNA–Dox–C_{60} fullerene hybrid system, weakly- and strongly-associated water clusters, Gibbs free energy, ^{1}H NMR spectroscopy.

1. Introduction

Doxorubicin (further referred as Dox) is a complex heterocyclic compound [1,2], poorly soluble in water and weakly polar organic solvents that is able to form inclusion compounds with the DNA molecules, and this determines the mechanism of its action on cancer cells [3]. Transdermal drug administering could be a promising way for treatment of tumors. To create composite/hybrid systems capable of effectively delivering medications through the skin, it is necessary for these systems to contain special additives that transform the interfacial water (intra- and extracellular) into a distinct clustered state [4]. It is possible to accomplish this by using mixtures of certain polar (e.g., DMSO) and nonpolar (e.g., aliphatic hydrocarbons) of organic compounds in combination with particles of highly dispersed silica and some types of biopolymer molecules (e.g., starch or DNA). In this case, it may be necessary to employ corrective nanoscale additives, such as water-soluble C_{60} fullerenes [5,6]. One can achieve the reduction of the desorption rate of Dox through noncovalent binding to DNA [7]. To investigate the structure of interfacial water clusters by low-temperature ^{1}H NMR spectroscopy in complex heterogeneous systems in the presence of the organic medium one should use aprotic solvents, such as CCl_4, instead of weakly polar (aliphatic) components.

We have previously shown that both the DNA and its adsorption complexes with silica exhibit the ability to structure hydrate water in a medium of weakly polar organic solvents in such a way that several signals of water

are recorded in the ^{1}H NMR spectra [7]. These signals correspond to the formation at phase boundaries of clusters with different average number of hydrogen bonds per each water molecule. Additional control of the surface properties in nanosilica/DNA-based composite can be achieved by introducing particles of nanocarbon material C_{60} fullerene into the surface layer [8]. The surface of C_{60} fullerene is formed by sp^2 hybridized carbon atoms [9], providing high lipophilicity and also the possibility for interaction between the electrodonor functional groups and the π-system of the C_{60} fullerene. Besides, the C_{60} fullerene alone as well as in combination with Dox demonstrates high antitumor activity [10–12], which may have a positive impact on the properties of many fullerene-containing medicinal compounds [13,14].

Thus, the aim of this work was to study the hydration properties of the hybrid adsorbent based on a nanosilica A-300, adsorptionally modified DNA and loaded with Dox as well as influence of C_{60} fullerene nanoparticles on properties of this system outlined above.

2. Experimental

2.1. Material

Highly dispersed silica (HDS, Aerosil A-300, Kalush Experimental Plant of the O.O. Chuiko Institute of Surface Chemistry of NAS of Ukraine) with a specific surface of 300 m^2/g was used as mineral component of the hybrid.

Highly stable water colloid C_{60} fullerene solution with concentration 1 mg/ml was prepared by transfer of C_{60} molecules (purity > 99.5%) from toluene to water using ultrasound sonication [6]. Theoretical calculations and experimental data (probe microscopy, dynamic light and small-angle neutron scattering measurements) show that the colloid solution of C_{60} fullerenes in water contain mainly both individual C_{60} molecules (~0.7 nm diameter) as well as their clusters (~2–100 nm diameter), in a hydrated state [10,11,15–19].

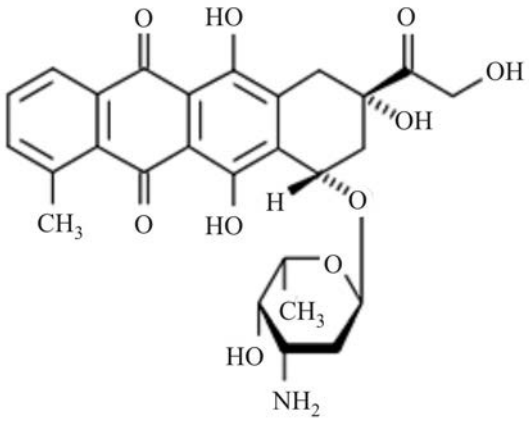

Fig. 1. Structural formula of the Dox molecule.

For the synthesis of the hybrid 0.2 g of DNA (Sigma, Germany) and 0.0015 g of Dox (Pharmacia & Upjohn, Italy; the structural formula of the Dox molecule is given on Fig. 1) were dissolved in 90 ml of distilled water and resulting solution was freeze-dried in vacuum. Afterwards, a mixture of the obtained complex (0.06 g) with Aerosil A-300 was mechanically activated in an agate mortar in the presence of a small amount of water. After of approximately 30 min of activation a biopolymer loaded with Dox uniformly covered the surface of the silica particles. This was accompanied by an increase in its bulk density from 50 up to 200 mg/g. Nanosilica presents in aqueous suspensions in the form of aggregates of 20–50 nm radius. During the creating SiO_2–DNA–Dox composite by mechano-chemical activation method the new aggregates form, in which one or more DNA molecules are surrounded by a nanoscale labile capsule consisting of silica particles. The process of formation of SiO_2–DNA–Dox aggregates is controlled by the minimum value of the free energy of the "silica–biopolymer" system. It can be argued that the content of DNA in it corresponds to 0.2–0.4 of statistical monolayer.

Placement of C_{60} molecule onto the surface of the hybrid particles of SiO_2–DNA–Dox was carried out by wetting them in a suspension of C_{60} fullerene in distilled water (~1 g per 100 mg SiO_2). This method provided an even surface distribution of C_{60} fullerene and its relatively high concentration in the hybrid (~0.8%) by weight relative to the mass of the solid.

2.2. ^{1}H NMR spectroscopy

NMR spectra were recorded on a high-resolution NMR spectrometer (Varian "Mercury") with an operating frequency of 400 MHz. 90 degrees 3 μs probe pulses were employed. The temperature in the sensor was regulated by a thermal control device Bruker VT-1000 with an accuracy of ±1 degree. The signal intensities were determined by fitting the spectra with multiple Gaussian peaks and then measuring the peak areas. We performed zero line and phase optimization with an accuracy, which for well-resolved peaks was not worse than 5%, and for overlapping peaks was ±10%. To prevent overcooling of water in the objects of interest, the concentration of unfrozen water was measured during heating of the samples pre-cooled to 210 K. The NMR measurement technique as well as the thermodynamic properties and the radii of the clusters of the interfacial water were described in detail in previous published papers [20–22].

During the analysis of the interfacial phenomena, to study the processes occurring at the solid–liquid–vapor interface two main approaches are employed — the method of excess Gibbs quantities and the method of a layer of finite thickness [23]. Within the former, it is assumed that the excess energy due to the formation of phase boundaries is concentrated in an infinitely thin surface layer, whereas the rest of the thermodynamic parameters of the fluid do

not differ from those of the bulk. In order to determine the geometric dimensions of the fluid volumes bounded by a solid surface, the following Gibbs–Thomson equation can be used that connects the relating radius (R) of the spherical or cylindrical water cluster with the magnitude of the freezing point depression:

$$\Delta T_m = T_m(R) - T_{m,\infty} = \frac{2\sigma_{sl} T_{m,\infty}}{\Delta H_f \rho R}, \qquad (1)$$

where $T_m(R)$ is the melting point of ice, localized in the pores of radius R; $T_{m,\infty}$ is the melting point of bulk ice; ρ is the density of the solid phase; σ_{sl} is the energy of the solid–liquid interaction and ΔH_f is the bulk enthalpy of fusion.

Equation (1) can be used to calculate the pore size distribution from the temperature dependence of the concentration of unfrozen water $C_{uw}(T)$. The latter is obtained by employing the ^{1}H NMR spectroscopy for layered water freeze-out for aqueous suspensions of solids or hydrated biological objects, when application of other methods for analysis of porous structures is quite difficult [24]. In practice, Eq. (1) can be used in a modified form $\Delta T_m = k/R$, where $k = 2\sigma_{sl} T_{m,\infty}/(\Delta H_f \rho)$ is a constant for many heterogeneous water-containing systems with magnitude of about 50 [22,24].

In the method of a layer of finite thickness [23] it is assumed that the effect of the interface extends over several molecular layers deep into the liquid phase. Then the process of freezing (or melting) of the interfacial water trapped in the solid porous matrix is occurring in accordance with the changes in Gibbs free energy (ΔG), due to the influence of the surface. This influence is decreasing away from the surface of the interface. At T = 273 K water freezes, with its properties similar to those of the bulk, and with further decrease of temperature (excluding the effects of over-freezing) freezing of water layers occurs very close to the surface. At that temperature, the following relation holds for the interfacial water

$$\Delta G_{\text{ice}} = -0.036\,(273.15 - T), \qquad (2)$$

where the numerical coefficient is a parameter related to the temperature coefficient of change in the Gibbs free energy for ice. Amounts of strongly- (SAW) and weakly-associated water (WAW), as well as the thermodynamic properties of these layers, can be calculated in accordance with the method described in detail in literature [20–22], in which the $C_{uw}(T)$ temperature dependence is determined from the signal intensity.

As was shown previously [20–22], the method of the low-temperature ^{1}H NMR spectroscopy with a liquid phase freeze-out allows calculating the amounts of associated water, its thermodynamic characteristics, and the size distribution of water-filled nanoscale cavities in macromolecules. The magnitude of the chemical shift in hydrogen atoms (δ_H) in the associated water determines the average number of H-bonds per water molecule. Since for the non-associated water (gas phase, solution in a weakly polar solvent) δ_H = 1–1.5 ppm, whereas for ice δ_H = 7 ppm [22,25], it can be concluded that the participation of water in the formation of one H-bond in H_2O as a proton donor and in another as an electron donor leads to an increase of δ_H by 2.7 ppm. Studies of various systems [20–22] have shown that within a certain hydrophobic-hydrophilic balance of the surface functional groups, water can transform into the WAW state represented by the protons signal at δ_H = 1–2 ppm. In this state, the average number of H-bonds per water molecule does not exceed 1 (out of 4 possible), otherwise the H-bond structure is strongly distorted compared to that of the bulk water since the decrease in the O–H...O angle leads to an increase in magnetic shielding of protons [26].

The measurements were performed in CCl_4 organic solvent medium. For the determination of the chemical shifts, tetramethylsilane (TMS) was used as internal standard (the concentration of TMS did not exceed 0.2 wt%).

3. Results and discussion

Figure 2 shows ^{1}H NMR spectra of water in SiO_2–DNA–Dox hybrids containing different amounts of water. The ^{1}H NMR spectra were recorded at different temperatures in CCl_4. Concentration of water in the original sample (Fig. 2(a)) was 5 mg/g. Varying the concentration was carried out in two ways: either by adding water to the slurry with a micro-dispenser (Fig. 2(b)) and its transfer to the adsorbent through the CCl_4 phase or by adding water to a dry powdered substance and equilibration of the sample through 10 min of vigorous shaking with a subsequent sustaining it in a vial for 1 h before adding CCl_4 (Fig. 2(c)). Dehydration of the initial sample was performed by heating it at 350 K for 10 min (Fig. 2(d)).

Figure 2 shows that water in the original hybrid sample can be observed as three signals with chemical shifts of 0.5–1.3 ppm (WAW) and 4–5 ppm (SAW). With rising temperature, there is an obvious shift of the signals toward stronger magnetic fields (smaller values of δ_H), which may be due to a decrease of association of water in clusters [20]. In the spectra the signal of TMS, which is added to CCl_4 as a standard reference, can be also observed.

The freezing point of the dispersive medium (CCl_4) is about 230 K. As it can be seen in Fig. 2, the interfacial water and TMS can be still observed in the spectra at lower temperatures. Consequently, the nonpolar medium, even after freezing, has little effect on the mobility of the TMS and water molecules. It is likely that a fraction of the organic medium in contact with the nanoparticles remains in unfrozen state, allowing water molecules that form the cluster structures to maintain both the rotational and the translational mobility. At the same time, the TMS molecules can congregate in nanoscale cavities, in which increasing concentrations of TMS lower the freezing point of CCl_4.

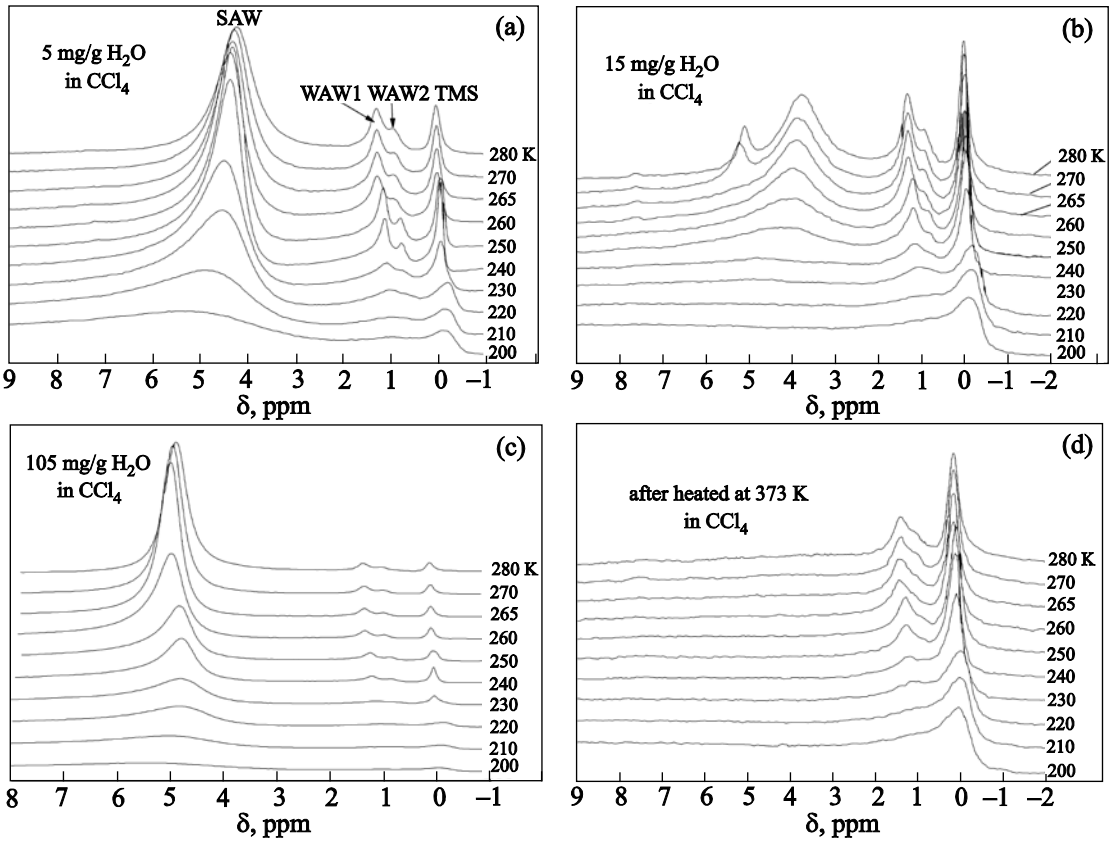

Fig. 2. ^{1}H NMR spectra of water in SiO_2–DNA–Dox hybrid recorded at different temperatures, various concentrations of interfacial water, as well as different processes of water addition.

WAW can be observed in the ^{1}H NMR spectra in two signals (WAW1 and WAW2). Similar spectra were also observed for WAW in both powdered solid DNA and DNA immobilized on silica nanoparticles [7]. Peculiarity of the system under study is in that both signals, WAW1 and WAW2, shift toward stronger magnetic fields with a decrease in temperature, whereas for solid DNA a significant shift into weaker magnetic fields was observed for the WAW1 signal, the intensity of which remains lower over the entire temperature range compared to that for the WAW2 signal. Probably, the differences should be attributed to the presence of Dox in the hybrid. The Dox molecules reduce the likelihood for the interfacial water molecules to participate in the formation of hydrogen-bonded complexes with electron-donating centers in the DNA molecules.

With the increase of water concentration (C_{H_2O}) up to 105 mg/g (Fig. 2(c)) there is a significant rise in the SAW signal intensity with a relatively weak change in the relative intensities of the WAW1, WAW2 and TMS signals. Thus, the amount of WAW depends primarily on the structural characteristics of the composite surface and changes rather insignificantly with the variation of C_{H_2O}.

With an addition of more water into the a sample through the organic solvent phase (Fig. 2(b)), the spectra change significantly compared to those shown in Fig. 3(a),(c) and SAW freezing occurs at a relatively higher temperature. At ~273 K two SAW signals are recorded in the spectra having different values of the chemical shift, with δ_H = 3–4 ppm for the main SAW signal indicating a significant decrease in the strength of association. The SAW signal vanishes for low magnetic fields at T < 270 K, therefore it is subject to fairly large water aggregates [24]. Most likely those are SAW microdroplets located near the phase boundaries of the composite particles. Due to its high viscosity, the colloidal system can remain in a non-equilibrium state for long time, however, the surface affinity of the composite particles to water remains high, as evidenced by the findings presented in Fig. 2. Thus, according to the findings shown in Fig. 2, the amount of water that can be administered into the hydrate shell of the composite can be increased six-fold.

Figure 2(d) shows ^{1}H NMR spectra obtained at different temperatures for a sample dehydrated by keeping it at T = 350 K. In these spectra there is practically no SAW signal, whereas the WAW signal intensity decreased by less than a factor of 2. Therefore, it can be concluded that all the WAW is strongly bound and its removal from the surface occurs at significantly greater energy loss than for SAW.

^{1}H NMR spectra obtained at different temperatures for the SiO_2–DNA–Dox–C_{60} fullerene hybrid samples are shown in Fig. 3. The weight concentration of C_{60} mole-

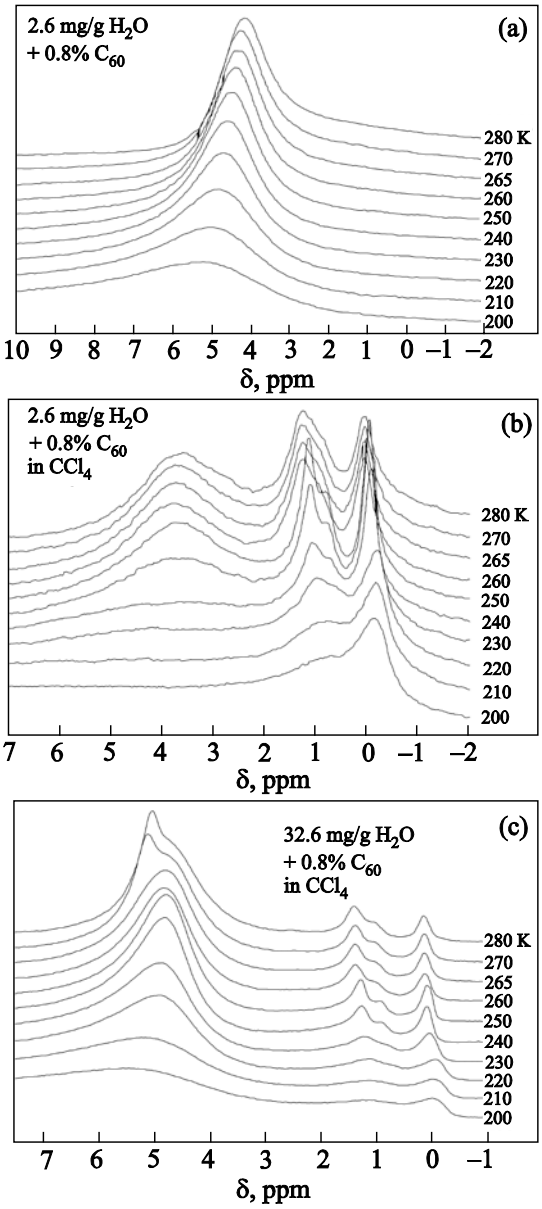

Fig. 3. ^{1}H NMR spectra of water in SiO_2–DNA–Dox–C_{60} fullerene hybrid recorded at different temperatures in air (a), CCl_4 ambient with C_{H_2O} = 5 mg/g (b), and CCl_4 ambient with C_{H_2O} = 32.6 mg/g (c).

cules in the composite was adjusted in order to be comparable to that of DNA. For the same sample the measurements were performed in air (Fig. 3(a)) and in CCl_4 ambient (Fig. 3(b)). Then additional amount of water has been introduced into the sample through the organic solvent phase (Fig. 3(c)).

From the comparison of the spectra shown in Fig. 3(a) and 3(b) it can be seen that the presence of weakly polar forms of water is largely determined by the presence of the weakly-polar organic solvent phase. Although in the original sample (Fig. 3(a)) there is a certain asymmetry of the signal (especially at ~273 K), which may be associated with the presence of a small amount of WAW, it is too weak to reveal itself as an isolated signal. The chemical shift of the SAW signal in air ambient changes from 5 ppm at 200 K to 4 ppm at 280 K due to the somehow weaker tendency of association of water with increasing temperature. The intensity of the water signal changes insignificantly demonstrating the strong binding of water to the surface of solid particles of the dispersed phase.

In the CCl_4 ambient the spectra change dramatically (Fig. 3(b)). At 280 K the SAW and WAW signals are observed in the spectra with similar intensities. The SAW signal has a chemical shift in the range of 3.2–4 ppm, i.e., the association of SAW is significantly lower than for the same sample in air. Another feature is the freezing of SAW at relatively high temperature (above 240 K). Thereby, according to published results [22] it should be classified as weakly bonded water. Introduction of additional amount of water into the colloidal system (Fig. 3(c)) leads to an increase in intensity of the SAW signal. Moreover, its intensity becomes less sensitive to temperature variations. Comparison of the spectra shown in Fig. 2(a) and 3(a) suggests that the transition of water into the WAW state is due primarily to the presence of the C_{60} fullerene nanoparticles.

Similarly to what was observed for the SiO_2–DNA–Dox hybrid (Fig. 2(b)) with the introduction of an additional amount of water through the nonpolar CCl_4 medium, SAW can be detected in the spectra shown in Fig. 3. This SAW, which has not penetrated into the adsorption layer of the composite particles, is present in the form of fairly large clusters or nanodomains. Such nonequilibrium aqua-aggregates can exist long enough (at least for several hours). Probably, they are stabilized by the confinement-related limitations for the diffusion of water within the interparticle space of the hybrid filled with CCl_4 toward the hydrophilic regions of the surface.

Figure 4 shows the temperature changes of SAW and WAW signal intensity at various water concentrations in the SiO_2–DNA–Dox and SiO_2–DNA–Dox–C_{60} fullerene hybrids. Figure 5 presents the distributions, calculated according to Eq. (1) and (2), of: (a) the sizes of adsorbed water clusters and (b) their energy of interaction with the phase boundaries. Since the measurements were performed in the temperature range of 200–280 K, for the fraction of water that remained in the unfrozen state it was provisionally assumed that it exists in the form of clusters with an average radius of 0.4 nm.

For SiO_2–DNA–Dox the $C_{SAW}(T)$ dependence (Fig. 4(a)) seems to be sensitive not only to the C_{H_2O} magnitude, but also to the method of introduction of additional portions of water. Thus, when C_{H_2O} = 15 mg/g for T < 240 K, the $C_{SAW}(T)$ curve lies below that one for a sample containing less water. This finding indicates a significant change in the size of water clusters and their energy of interaction with the interface. Indeed, from Fig. 5, it can be seen that when C_{H_2O} = 5 mg/g, water is in the form of clusters smaller than 5.1 nm, whereas when C_{H_2O} = 15 mg/g the

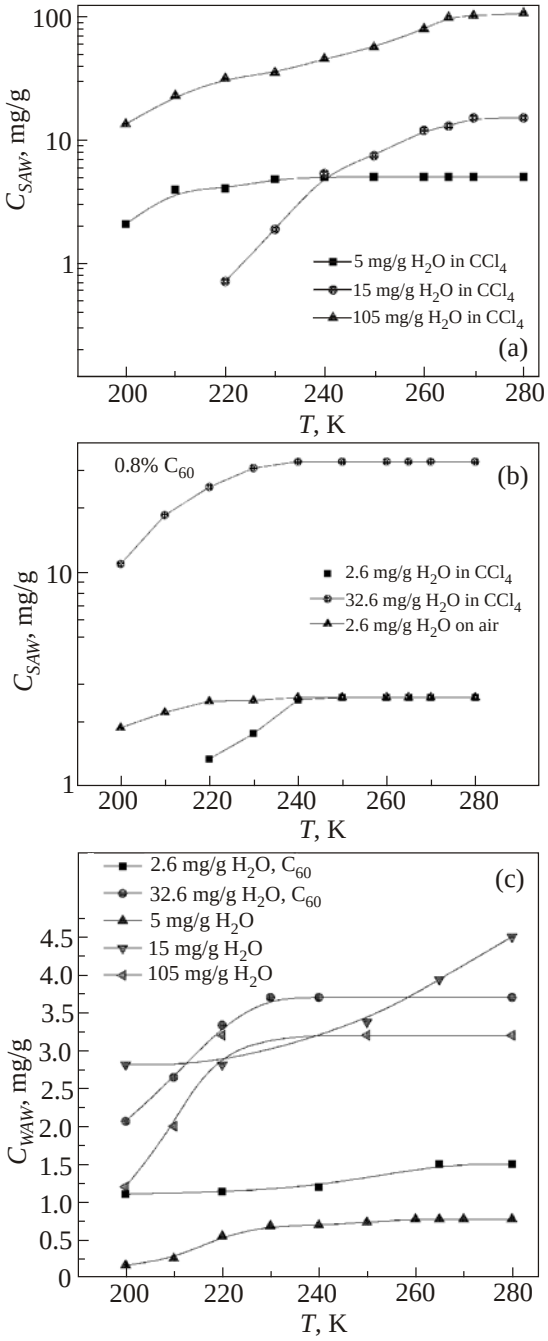

Fig. 4. Temperature dependences for the concentration of SAW (a), (b) and WAW (c) for the SiO_2–DNA–Dox and SiO_2–DNA–Dox–C_{60} fullerene hybrids.

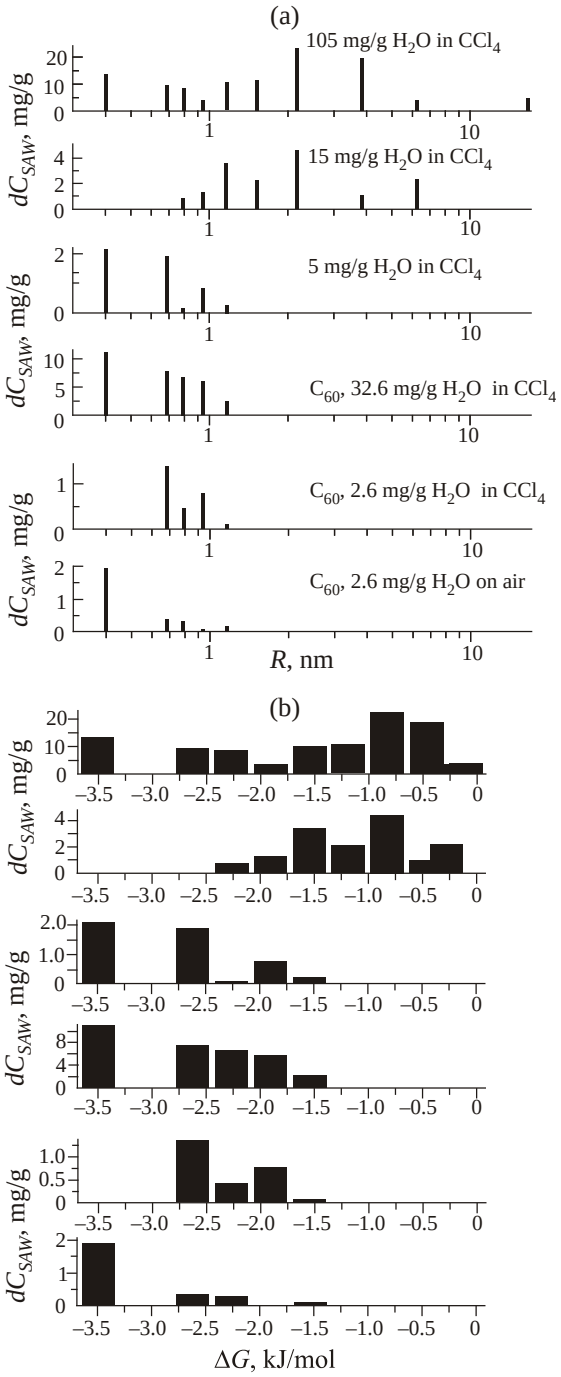

Fig. 5. Cluster radius distribution (a) and distribution of the changes (b) in the Gibbs free energy due to adsorption interactions for clusters of adsorbed water.

range of cluster sizes is 0.8–5.5 nm. Hence, the decrease in the Gibbs free energy due to the adsorption interactions for the initial sample (C_{H_2O} = 5 mg/g) is the greatest and reaches –3.5 kJ/mol, while for the sample in which the water content is increased by introduction through the organic phase (C_{H_2O} = 15 mg/g), the decrease in the Gibbs free energy does not exceed –2.25 kJ/mol (Fig. 5(b)). When balancing the sample with an additional portion of water in air (C_{H_2O} = 105 mg/g) one can observe in the $dC_{SAW}(R)$ and $dC_{SAW}(\Delta G)$ distributions, water clusters the sizes of which vary across the entire measurable range, while the ΔG magnitude can exceed –3.5 kJ/mol (such water freezes at $T < 200$ K).

For the SiO_2–DNA–Dox–C_{60} fullerene hybrid the $C_{SAW}(T)$ dependence at constant C_{H_2O} changes substantially when air ambient is replaced with CCl_4 (Fig. 4(b)). For $T < 240$ K, the slope increases significantly due to easing of water solidification under the influence of nonpolar

organic medium. As a result, the average radius of water clusters increases from 0.4 to 0.8 nm (Fig. 5(a)), while a lowering of the Gibbs free energy from –3.5 to –2.25 kJ/mol (Fig. 5(b)) occurs.

Similar effect was previously observed for many types of carbon materials and certain types of mesoporous silica [21,22]. It occurs because during the formation of SAW clusters on a weakly hydrophilic surface they interact with the surface by forming a relatively small number of hydrogen bonds. At the same time, they interact, as a whole system, with the surface via dispersion interactions. In the case of shared adsorption of water and excess nonpolar substance at the surface the effectiveness of dispersion interactions with the organic phase is higher than with water. As a result, CCl_4 penetrates into the narrow gap between the clusters and the SAW surface, reducing in this way the binding energy of the SAW clusters due to increasing distance from the surface. According to Fig. 4(b), the average size of water clusters increases in the presence of CCl_4. It is accompanied by a simultaneous decrease in the number of small SAW clusters.

For both hybrid materials (SiO_2–DNA–Dox and SiO_2–DNA–Dox–C_{60}), WAW can be described as tightly bound because it freezes at $T < 250$ K [21]. The only exception is the SiO_2–DNA–Dox sample with water added through the CCl_4 phase (Fig. 4(c)). One can assume that WAW is stabilized by the organic environment and exists in the form of small clusters, in which water molecules interact with each other mainly via the dipole–dipole mechanism. Furthermore, such structures are formed with the participation of not only the active surface centers, but also the CCl_4 molecules.

According to Eq. (1), the WAW cluster size should not exceed 1.2 nm, but however in the present study a reliable determination of the structure of these clusters was not able to be done.

4. Conclusions

Properties of interfacial water in a hybrid created by an adsorptive attachment of DNA–Dox at the surface of A-300 silica differ significantly from the hydration properties of the SiO_2–DNA system. In CCl_4 medium, ^1H NMR SAW signals are measured at the surface as well as two types of WAW signals. However, no signal is observed for water associated with electron-donor centers of DNA molecules, which are otherwise detected in solid powdered DNA. This probably occurs due to a significant change in the structure of interfacial water clusters resulting in accelerated molecular exchange between different types of adsorbed water.

Inclusion of C_{60} fullerene nanoparticles into the SiO_2–DNA–Dox hybrid in CCl_4 ambient reduces interaction of SAW clusters with the surface, due to certain distance between the clusters and the surface, as well as due to the change in the cluster size distribution (trending toward formation of larger water clusters). It is, thus, possible to control the hydration properties of the Dox-loaded SiO_2–DNA hybrid, and, in particular, the abundance and size ratio of the WAW/SAW clusters.

It was found that the addition of water into the colloidal system based on the SiO_2–DNA–Dox and SiO_2–DNA–Dox–C_{60} fullerene hybrids and CCl_4 leads to the formation in them of long-lived nonequilibrium submicron size water clusters, which are weakly bound to the surface of the particles and affect significantly their hydration properties.

1. S. Hrelia, D. Fiorentini, T. Maraldi, C. Angeloni, A. Bordoni, P.L. Biagi, and G. Hakim, *Biochem. Biophys. Acta* **64**, 139 (2002).
2. M.A.I. Abou El Hassan, H.M.W. Verheul, A.S. Jorna, C. Schealkwijk, J. van Bezu, W.J.F. van der Vijgh, and A. Bast, *British J. Cancer* **98**, 357 (2003).
3. *Cancer: Principles and Practice of Oncology*, V.T. de Vita, S. Hellman, and S.A. Rosenberg (eds.), Lippincott Williams and Wilkins, Philadelphia (2001).
4. V.V. Turov and V.M. Gun'ko, *Clustered Water and Ways of its Application*, Naukova Dumka, Kiev (2011).
5. P. Scharff, K. Risch, L. Carta-Abelmann, I.M. Dmytruk, M.M. Bilyi, O.A. Golub, A.V. Khavryuchenko, E.V. Buzaneva, V.L. Aksenov, M.V. Avdeev, Yu.I. Prylutskyy, and S.S. Durov, *Carbon* **42**, 1203 (2004).
6. S.V. Prylutska, O.P. Matyshevska, I.I. Grynyuk, Yu.I. Prylutskyy, U. Ritter, and P. Scharff, *Mol. Cryst. Liq. Cryst.* **468**, 265 (2007).
7. V.V. Turov, V.F. Chehun, V.N. Barvinchenko, T.V. Krupskaya, Yu.I. Prylutskyy, U. Ritter, and P. Scharff, *J. Mater. Sci.: Mater. Med.* **22**, 525 (2011).
8. V.V. Turov, V.F. Chehun, T.V. Krupskaya, V.N. Barvinchenko, S.V. Chehun, A.P. Ugnivenko, Yu.I. Prylutskyy, P. Scharff, and U. Ritter, *Chem. Phys. Lett.* **496**, 152 (2010).
9. A. Hirsch, *The Chemistry of Fullerenes*, Thieme Publishing Group, Studtgart (1994).
10. S.V. Prylutska, A.P. Burlaka, Yu.I. Prylutskyy, U. Ritter, and P. Scharff, *Exp. Oncol.* **33**, 162 (2011).
11. S.V. Prylutska, A.P. Burlaka, P.P. Klymenko, I.I. Grynyuk, Yu.I. Prylutskyy, Ch. Schuetze, and U. Ritter, *Cancer Nanotechnol.* **2**, 105 (2011).
12. S.V. Prylutska, A.P. Burlaka, Yu.I. Prylutskyy, U. Ritter, and P. Scharff, *Biotechnol.* **4**, 82 (2011).
13. A.S. Buchelnikov, V.V. Kostyukov, M.P. Yevstigneev, and Yu.I. Prylutskyy, *Russ. J. Phys. Chem. A* **87**, 662 (2013).
14. M.P. Evstigneev, A.S. Buchelnikov, D.P. Voronin, Yu.V. Rubin, L.F. Belous, Yu.I. Prylutskyy, and U. Ritter, *Chem. Phys. Chem.* **14**, 568 (2013).
15. Yu.I. Prilutski, S.S. Durov, V.N. Yashchuk, T.Yu. Ogul'chansky, V.E. Pogorelov, Yu.A. Astashkin, E.V. Buzaneva, Yu.D. Kirghizov, G.V. Andrievsky, and P. Scharff, *Eur. Phys. J. D* **9**, 341 (1999).
16. L. Bulavin, I. Adamenko, Yu. Prylutskyy, S. Durov, A. Graja, A. Bogucki, and P. Scharff, *Phys. Chem. Chem. Phys.* **2**, 1627 (2000).

17. Yu.I. Prylutskyy, S.S. Durov, L.A. Bulavin, I.I. Adamenko, K.O. Moroz, I.I. Geru, I.N. Dihor, P. Scharff, P.C. Eklund, and L. Grigorian, *Int. J. Thermophys.* **22**, 943 (2001).
18. N.O. Mchedlov-Petrossyan, *Chem. Rev.* **113**, 5149 (2013).
19. Yu.I. Prylutskyy, A.S. Buchelnikov, D.P. Voronin, V.V. Kostjukov, U. Ritter, J.A. Parkinson, and M.P. Evstigneev, *Phys. Chem. Chem. Phys.* **15**, 9351 (2013).
20. V.V. Turov and R. Leboda, *Adv. Colloid. Interface Sci.* **79**, 173 (1999).
21. V.M. Gun'ko, V.V. Turov, V.M. Bogatyrev, V.I. Zarko, R. Leboda, E.V. Goncharuk, A.A. Novza, A.V. Turov, and A.A. Chuiko, *Adv. Colloid. Interface Sci.* **118**, 125 (2005).
22. .M. Gun'ko, V.V. Turov, and P.P. Gorbik, *Water at the Interface*, Naukova Dumka, Kiev (2009).
23. Yu.G. Frolov, *Course of Colloid Chemistry. Surface Phenomena and Disperse Systems, Chemistry*, Moscow (1988).
24. O.V. Petrov and I. Furo, *Progr. NMR Spectr.* **54**, 97 (2009).
25. D.R. Kinney, I.S. Chaung, and G.E. Maciel, *J. Am. Chem. Soc.* **115**, 6786 (1993).
26. V.M. Gun'ko and V.V. Turov, *Langmuir* **15**, 6405 (1999).